The Astrophysical Journal, 695:679–694, 2009 April 10 doi:10.1088/0004-637X/695/1/679

STELLAR ROTATION IN M35: MASS–PERIOD RELATIONS, SPIN-DOWN RATES, AND GYROCHRONOLOGY*

Søren Meibom[1,3,4], Robert D. Mathieu[1,4], and Keivan G. Stassun[2,4]
Department of Astronomy, University of Wisconsin-Madison, Madison, WI 53706, USA; smeibom@cfa.harvard.edu
Physics and Astronomy Department, Vanderbilt University, Nashville, TN 32735, USA
Received 2008 May 2; accepted 2009 January 13; published 2009 April 1

ABSTRACT

We present the results of a five month photometric time-series survey for stellar rotation over a $40' \times 40'$ field centered on the 150 Myr open cluster M35. We report rotation periods for 441 stars within this field and determine their cluster membership and binarity based on a decade-long radial velocity survey, proper-motion measurements, and multiband photometric observations. We find that 310 of the stars with measured rotation periods are late-type members of M35. The distribution of rotation periods for cluster members span more than 2 orders of magnitude from ∼0.1 to 15 days, not constrained by the sampling frequency and the timespan of the survey. With an age between the zero-age main sequence and the Hyades, and with ∼6 times more rotation periods than measured in the Pleiades, M35 permit detailed studies of early rotational evolution of late-type stars. Nearly 80% of the 310 rotators lie on two distinct sequences in the color–period plane, and define clear relations between stellar rotation period and color (mass). The M35 color–period diagram enables us to determine timescales for the transition between the two rotational states, of ∼60 Myr and ∼140 Myr for G and K dwarfs, respectively. These timescales are inversely related to the mass of the convective envelope, and offer constraints on the rates of internal and external angular momentum transport and of the evolution of stellar dynamos. A comparison to the Hyades, confirm the Skumanich spin-down dependence for G dwarfs on one rotational state, but suggest that K dwarfs spin down more slowly. The locations of the rotational sequences in the M35 color–period diagram support the use of rotational isochrones to determine ages for coeval stellar populations. We use such gyrochronology to determine "gyro-ages" for M35 from 134 Myr to 161 Myr. We use the M35 data to evaluate new color dependences for the rotational isochrones.

Key words: open clusters and associations: individual (M35) – stars: evolution – stars: late-type – stars: rotation

Online-only material: color figures, extended figure, machine-readable table

1. INTRODUCTION

Observations of coeval populations of late-type stars younger than the Hyades have revealed that they rotate with periods ranging over 2 orders of magnitude—from near-breakup to periods similar to the Sun. Understanding why some stars deplete their angular momentum faster than others, which physical processes are at work, when, and to what extent, is a primary mandate for stellar evolution research.

The discovery from photometric and spectroscopic measurements in the Pleiades of sub 1 day rotation periods for K dwarfs (Alphenaar & van Leeuwen 1981; van Leeuwen & Alphenaar 1982; Meys et al. 1982; Soderblom et al. 1983) challenged prior understanding of the early angular momentum evolution for late-type stars, and sparked a renewed interest in the topic. Observations of mainly projected rotation velocities ($v \sin(i)$) of late-type stars in α Persei (50 Myr; Stauffer et al. 1985, 1989), the Pleiades (100 Myr; Soderblom et al. 1983, 1993a; Stauffer et al. 1984; Benz et al. 1984; Stauffer & Hartmann 1987; Terndrup et al. 2000), and the Hyades (625 Myr; Soderblom 1982; Benz et al. 1984; Radick et al. 1987), and photometric studies of the Hyades (Lockwood et al. 1984; Radick et al. 1987), confirmed the coexistence of slowly and rapidly rotating stars in α Persei and the Pleiades, but found an absence of rapid rotators in the Hyades. Furthermore, the rapid rotators in the youngest clusters were found primarily among K and M dwarfs and not among G dwarfs.

The emerging evidence for an age and mass dependence of rapid rotation prompted new ideas about the rotational evolution of late-type stars. For example, the suggestion of epochs of decoupling and recoupling of the stellar core and envelope (e.g., Stauffer et al. 1984; Soderblom et al. 1993b; Jianke & Collier Cameron 1993). The idea of decoupling—allowing the more shallow convective envelope of G dwarfs to spin down faster than the envelopes in K and M dwarfs—had developed in parallel in models of stellar rotation (e.g., Endal & Sofia 1981; Pinsonneault et al. 1990; MacGregor & Brenner 1991; Barnes & Sofia 1996). However, the concept of decoupling, if permanent, is in conflict with helioseismic observations of the Sun as a solid-body rotator (Gough 1982; Duvall et al. 1984; Goode et al. 1991; Eff-Darwich et al. 2002). Furthermore, recoupling—giving access to the angular momentum reservoir of the faster spinning core—was suggested by Soderblom et al. (1993b) as being necessary to explain the evolution beyond the age of the Pleiades of slowly rotating stars (Soderblom et al. 1993b).

Understanding the formation of the rapid rotators is a separate problem. The fastest spinning stars in the youngest clusters cannot be explained from Skumanich-style spin-down (Skumanich 1972) of the fastest spinning T Tauri stars. The rapid rotators can be explained only by introducing "magnetic saturation"

* WIYN Open Cluster Study. XXXV.

[3] Now at Harvard–Smithsonian Center for Astrophysics, Cambridge, MA 02138, USA.

[4] Visiting Astronomer, Kitt Peak National Observatory, National Optical Astronomy Observatory, which is operated by the Association of Universities for Research in Astronomy, Inc. (AURA) under cooperative agreement with the National Science Foundation.

of the angular momentum loss via stellar winds (Stauffer & Hartmann 1987; MacGregor & Brenner 1991; Barnes & Sofia 1996; Bouvier et al. 1997; Krishnamurthi et al. 1997; Sills et al. 2000), and by allowing the saturation threshold to depend on the stellar mass. The physical meaning of "saturation" is still unclear.

During the pre-main-sequence (PMS) phase, large dispersions and substructure (bimodalities) in the rotation-period distributions has also been observed for coeval stellar populations. Here, a popular explanation for coeval rapid and slow rotators originates from the work of Koenigl (1991) and Edwards et al. (1993) on interactions between T Tauri stars and their circumstellar disks. "Magnetic disk-locking" was introduced to provide a means to brake the spin-up of the central star by transferring angular momentum from the star to the disk (e.g., Shu et al. 1994; Najita 1995, and references therein). Accordingly, rotation-period dispersions (bimodalities) should result if some stars lose their disks faster than others (e.g., weak versus classic T Tauri stars). Whether magnetic disk-braking is a dominant process regulating stellar rotation during the early PMS remains under debate on both observational and theoretical grounds.

Recently, taking advantage of results from an increasing number of photometric monitoring programs of late-type stars in young main-sequence clusters, Barnes (2003) presented an interpretation of his own and other published rotation period data. Free of the ambiguities of $v \sin(i)$, Barnes identified, in each coeval stellar population, separate groups of fast and intermediate/slowly rotating stars with different dependences on color (mass). He specifically proposed that coeval stars fall along two "rotational sequences" in the color versus rotation period plane. From an analysis of these sequences and their dependences on stellar age, Barnes (2003) proposed a framework for connecting internal and external magnetohydrodynamic processes to explain the evolution in the observed period distributions, including bimodalities. This approach combines the ideas of (e.g., Stauffer et al. 1984; Soderblom et al. 1993b) of an initial decoupling of the stellar core and envelope with reconnection of the two zones through a global dynamo-field at a later and mass-dependent time. It does not (yet) interface with PMS angular momentum evolution. Importantly, Barnes (2003) also proposed that the age dependence of the location of the rotational sequences in the color–period plane, could be used to measure the age of a stellar population, much like the sequences in the color–magnitude diagram (CMD). Barnes (2007) further developed this idea of "gyrochronology." Determining the age of a late-type star from its rotation and color, had previously been suggested by Kawaler (1989).

Interpretation aside, it has become desirable and increasingly possible to eliminate the ambiguity of projected rotation velocities ($v \sin(i)$) by measuring photometric rotation periods from light modulation by spots on the surfaces of young late-type stars. While more labor and time intensive, photometric measurements of rotation periods in coeval populations, promise to reveal important details about dependences of rotation on other stellar properties—most obviously mass and age, but likely also stellar activity, internal/external magnetic configurations, and binarity.

We present in this paper the results of an extensive time-series photometric survey for rotation periods and a decade-long spectroscopic surveys for membership and binarity for late-type stars in the field of the open cluster M35 (NGC 2168). The combination of time-series and multiband photometry with time-series radial velocity data enable us to explore the distribution of rotation periods versus stellar color (mass) for bona fide single and binary members of M35.

M35 is a rich ($\gtrsim$2500 stars; Barrado y Navascués et al. 2001) northern hemisphere cluster located ~800–900 pc (Barrado y Navascués et al. 2001; Kalirai et al. 2003) toward the galactic anticenter ($\alpha_{2000} = 6^{\rm h}9^{\rm m}$, $\delta_{2000} = 24^\circ20'$; $l = 186\overset{\circ}{.}59$, $b = 2\overset{\circ}{.}19$). The age of M35 has been estimated to 150 Myr (von Hippel et al. 2002), 175 Myr (Barrado y Navascués et al. 2001), and 180 Myr (Kalirai et al. 2003). We adopt an age of 150 Myr, in agreement with the most recent age determination based on the isochrone method (C. P. Deliyannis 2008, private communication). At the distance of M35, the majority of cluster members are confined to within a ~$0\overset{\circ}{.}5$ diameter field, facilitating photometric and spectroscopic observations of a large number of stars through wide-field CCD imaging and multiobject spectroscopy. Older and much more populous than the Pleiades, and younger than the Hyades, M35 nicely bridges a gap in the age sequence of star clusters with comprehensive information about rotation and membership, permitting a more detailed study of the rotational evolution of late-type stars beyond the zero-age main sequence (ZAMS).

We begin in Section 2 by describing our time-series photometric observations, our methods for data-reduction and for photometric period detection, and the information about cluster membership available from our spectroscopic survey and the M35 CMD. In Section 3, we present the distribution of rotation periods in M35, discuss the short- and long-period tails in the context of our period-detection limits, and assess the stability/lifetime of spots or groups of spots by comparison of our short- and long-term photometric data. Section 4 introduces the M35 color–period diagram and the observed dependences of stellar rotation on mass. In Section 5, we discuss and interpret the M35 color–period diagram in the context of present ideas for stellar angular momentum evolution. In particular, we use the diagram to estimate spin-down rates for G and K dwarfs, to test the time dependence on rotational evolution from a comparison with measured rotation periods in the Hyades, to determine M35's gyrochronology age, and to evaluate the best functional representation of the color–period dependence in the M35 data. Section 6 summarizes and presents our conclusions.

2. OBSERVATIONS, DATA REDUCTION, AND METHODS

2.1. Time-series Photometric Observations

We photometrically surveyed stars in a region approximately $40' \times 40'$ centered on the open cluster M35 over a timespan of 143 days. The photometric data were obtained in the Johnson V band with the WIYN[5] 0.9 m telescope[6] on Kitt Peak equipped with a $2k \times 2k$ CCD camera. The field of view of this instrument is $20\overset{'}{.}5 \times 20\overset{'}{.}5$ and observations where obtained over a 2×2 mosaic.

The complete data set presented is composed of images from high-frequency (approximately once per hour for 5–6 hours per night) time-series photometric observations over 16 full nights during 2002 December 2–17, complemented with a queue-scheduled observing program over 143 nights from 2002 October 22 to 2003 March 11, obtaining one image per night

[5] The WIYN Observatory is a joint facility of The University of Wisconsin-Madison, Indiana University, Yale University, and the National Optical Astronomy Observatory (NOAO).

[6] The 0.9 m telescope is operated by WIYN Inc. on behalf of a Consortium of 10 partner universities and organizations (see http://www.noao.edu/0.9m/general.html).

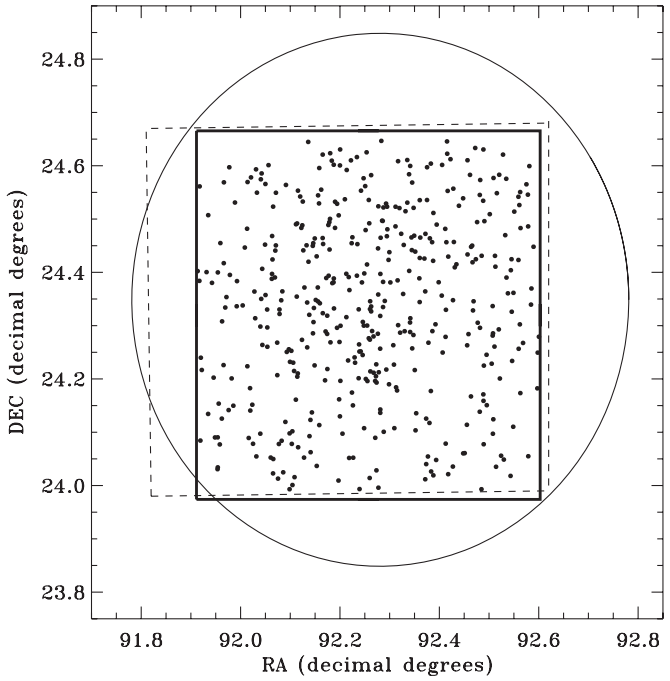

Figure 1. Locations and spatial extents of the photometric and spectroscopic surveys used in this study. The innermost solid square denotes the $40' \times 40'$ region of our time-series photometric survey. Within it we show the distribution of the 441 stars with measured rotation periods (black dots). The dashed rectangle displays the region of the multiband photometric study by C. P. Deliyannis (2008, private communication) and the circle represents the 1° diameter field of our spectroscopic survey of M35 (Meibom & Mathieu 2005).

interrupted only by bad weather and scheduled instrument changes. The result is a database of differential *V*-band light curves for more than 14,000 stars with $12 \lesssim V \lesssim 19.5$. The sampling frequency of the 2002 December observations allow us to detect photometric variability with periods ranging from less than a day to about 10 days. The long timespan of the queue-scheduled observations provide data suitable for detecting periodic variability of up to ~75 days, and for testing the long-term stability of short-period photometric variations. From this database, we derive rotation periods for 441 stars.

Figure 1 shows the surveyed region (solid square) and the spatial distribution of the 441 rotators. The region is roughly coincident with that of C. P. Deliyannis (2008, private communication) in which they obtained *UBVRI* CCD photometry for ~19,000 stars (dashed square). Also shown is the circular target region of our spectroscopic survey described in Section 2.4 and in Meibom & Mathieu (2005). The photometric survey was carried out within the region of the spectroscopic survey to optimize information about spectroscopic membership and binarity.[7]

Figure 2 displays the time-series data from both programs for a photometrically nonvariable star. Filled symbols represent the high-frequency observations and open symbols represent the queue-scheduled observations.

2.2. Basic Reductions, PSF Photometry, and Light Curves

Basic reductions of our CCD frames, identification of stellar sources, and computations of equatorial coordinates[8] were done using standard IRAF packages. Instrumental magnitudes were determined from point-spread function (PSF) photometry using the IRAF DAOPHOT package. The analytical PSF and a residual lookup table were derived for each frame based on ~30 evenly distributed isolated stars. The number of measurements in the light curve of a given star vary because stars near the edges of individual frames may be missed due to telescope pointing errors, while bright stars near the CCD saturation limit and faint stars near the detection threshold may be excluded on some frames because of variations in seeing, sky brightness, and sky transparency. To ensure our ability to perform reliable time-series analysis on stars in our database, we have eliminated stars that appear on fewer than half of the total number of frames. The resulting database contains 14,022 stars with a minimum of 75 measurements.

We applied the Honeycutt (1992) algorithm for differential CCD photometry to our raw light curves to remove nonstellar frame-to-frame photometric variations. We favor this technique for differential photometry because it does not require a particular set of comparison stars to be chosen a priori, nor does it require a star to appear in every frame. Figure 2 shows the light curve for a $V \sim 14$th magnitude star. The standard deviation from 157 photometric measurements is $0^m.004$, representative of our photometric precision at that brightness. Figure 3 shows the standard deviation of the photometric measurements as a function of the *V* magnitude for each star in the field of M35. The relative photometric precision is ~0.5% for stars with $12 \lesssim V \lesssim 14.5$.

2.3. Photometric Period Detection

We employed the Scargle (1982) periodogram analysis to detect periodic variability in the light curves because of its ability to handle unevenly sampled data. We searched a grid of 5000 frequencies corresponding to periods between 0.1 day and 90 days. The lower search limit was set at a period ensuring critical sampling based on the Nyquist critical frequency for our high-frequency data ($f_c = 1/(2\delta t)$), where δt is the sampling interval of ~1 hr. The upper limit was set at 90 days because a star with a 90 day period would complete about 1.5 cycle over the 143 nights of the survey.

A false alarm probability (FAP), the probability that a signal detected at a certain power level can be produced by statistical fluctuation, was calculated as the measure of confidence in a detected period. An analytical expression for estimating a FAP is given by Scargle (1982) and Horne & Baliunas (1986). However, these methods are not entirely suitable when applied to time-series photometric studies of young stars because they only test against random fluctuations of a purely statistical nature (i.e., measurement errors) and do not account for correlated fluctuations intrinsic to the source such as variability on timescales long compared to the sampling frequency. For young stars our repeated measurements during a single night are not necessarily independent and uncorrelated. Consequently, the analytical expressions estimating a FAP will likely overestimate the significance of any measured periodic variability. Hence, we performed a two-dispersion Monte Carlo calculation to estimate the FAP of our detected periods, as per Herbst & Wittenmyer (1996) and Stassun et al. (1999). For each star, we generated a set of 100 synthetic light curves, each consisting of normally distributed noise with two dispersions: one representing the variability of the star during a night and one representing the night-to-night variability of the star. The former was estimated by taking the mean of each night's standard

[7] All of these mutually supportive studies are part of the WIYN Open Cluster Study (WOCS; Mathieu 2000).

[8] We used data from the STScI Digitized Sky Survey; The Digitized Sky Surveys were produced at the Space Telescope Science Institute under U.S. Government grant NAG W-2166.

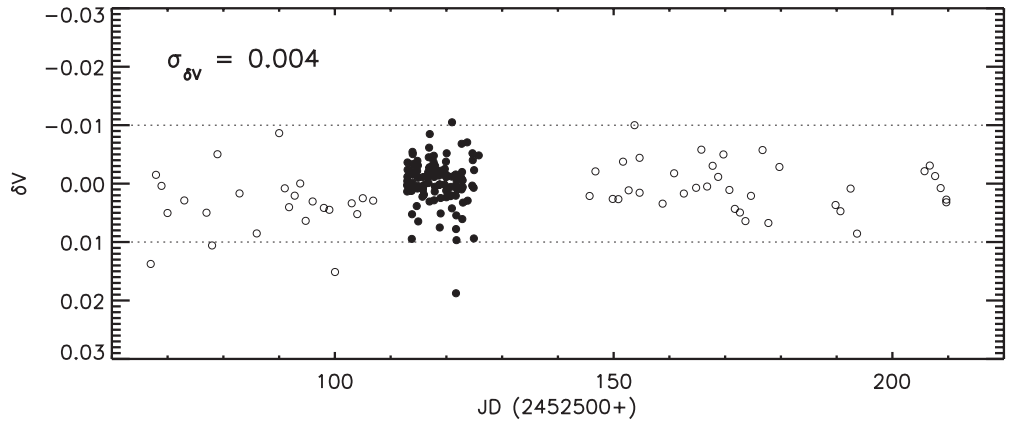

Figure 2. Sample time-series data from our photometric database for a nonvariable $V \simeq$ 14th magnitude star. Filled symbols represent measurements from the high-frequency 2002 December observing run and open symbols represent the low-frequency queue-scheduled observations. The data span a total of 143 days. The star was observed in all the 157 images of the northeast quadrant of the 2×2 mosaic. The standard deviation ($\sigma_{\delta V}$) of the 157 measurements is $0\overset{m}{.}004$, representative of our best photometric precision. The horizontal dotted lines denote $\delta V = \pm 0\overset{m}{.}01$.

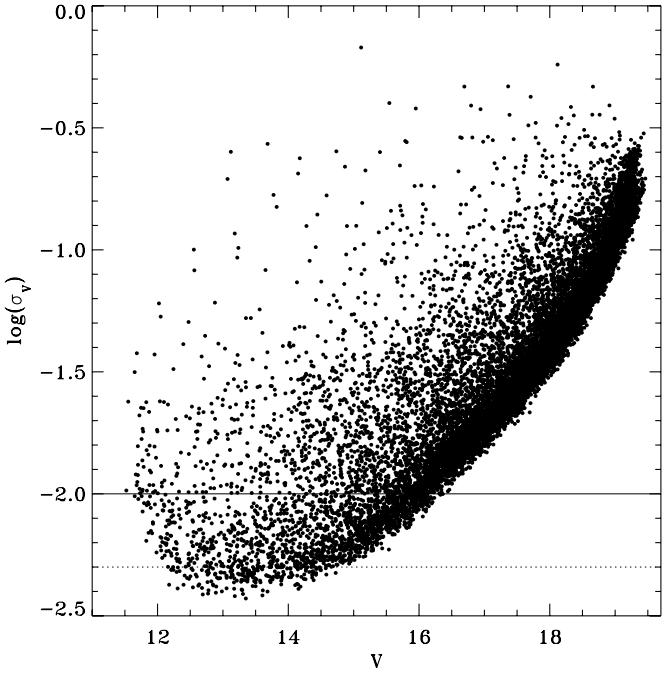

Figure 3. Logarithm of the standard deviation of all instrumental magnitudes as a function of V magnitude for 14,022 stars in the field of M35. The number of measurements for each star range from 75 to 216. The solid and dashed horizontal lines represent σ_V of 0.01 (1%) and 0.005 (0.5%), respectively. A relative photometric precision of ∼0.5% is obtained for stars with $12\overset{m}{.}0 \lesssim V \lesssim 14.5\overset{m}{.}0$.

deviation, and the latter by taking the standard deviation of nightly means. With this approach, the test light curves can vary on timescales that are long compared to our sampling interval, allowing them to mimic the random slow variability of stellar origin that could produce spurious periodic behavior over our limited observing window. The maximum power of the 100 periodograms of the test light curves was adopted as the level of 1% FAP, and used as the initial threshold for detecting significant photometric variability. For all stars that met the FAP criterion we examined (by eye) the periodogram and raw and phased light curves. We report stellar rotation periods for 441 stars in our database (see Table 1 in Appendix B).

We do not have multiple seasons of observations or observations in multiple pass-bands at our disposal by which to confirm rotation periods of individual stars. However, the reliability of the derived periods is supported by an observed correlation between photometric period and rotational line broadening within a subset of 16 single cluster members. Figure 4 shows the projected rotation velocities measured by Barrado y Navascués et al. (2001) for 16 stars for which we have determined rotation periods. The shortest period stars ($P_r \lesssim 2.5$ days) show increasing $v \sin(i)$ with decreasing rotation period. For rotation periods of ∼4 days or longer the upper limits on the projected rotation velocities are consistent with slower rotation. For comparison, the solid, dashed, and dotted curves in Figure 4 indicate the relation between rotation period and the projected rotational velocity for a solar-like star with a 90°, 70°, and 50° inclination of the rotational axis, respectively. Thus, for all the 16 stars, the projected rotation velocities are consistent with the measured rotation periods.

2.4. The Spectroscopic Survey

M35 has been included in the WOCS (Mathieu 2000) since 1997. As part of WOCS, more than 6000 spectra has been obtained of approximately 1500 solar-type stars within a 1° field centered on M35. The selection of survey target stars was based on photometric (C. P. Deliyannis 2008, private communication; see Section 2.5) and proper-motion (McNamara & Sekiguchi 1986; Cudworth 1971) membership data. Stars on or less than $\sim 1\overset{m}{.}0$ above the cluster main sequence were selected, with brightness and color ranges corresponding to a range in mass from ∼0.7 $M_\odot$ to ∼1.4 $M_\odot$. All spectroscopic data were obtained using the WIYN 3.5 m telescope equipped with a multiobject fiber optic positioner (Hydra) feeding a bench mounted spectrograph. Observations were done at central wavelengths of 5130 Å or 6385 Å with a wavelength range of ∼200 Å providing many narrow absorption lines. Radial velocities with a precision of $\lesssim$0.5 km s^{-1} (Geller et al. 2008; Meibom et al. 2001) were derived from the spectra via cross-correlation with a high signal-to-noise ratio sky spectrum. From this extensive radial velocity survey, we have (1) calculated the cluster membership probability, (2) detected the cluster binary stars, and (3) determined the orbital parameters for the closest binaries.

Of the 441 stars with rotation periods presented in this study, 259 have one or more radial velocity measurements (the remainder being below the faint limit of the spectroscopic survey or

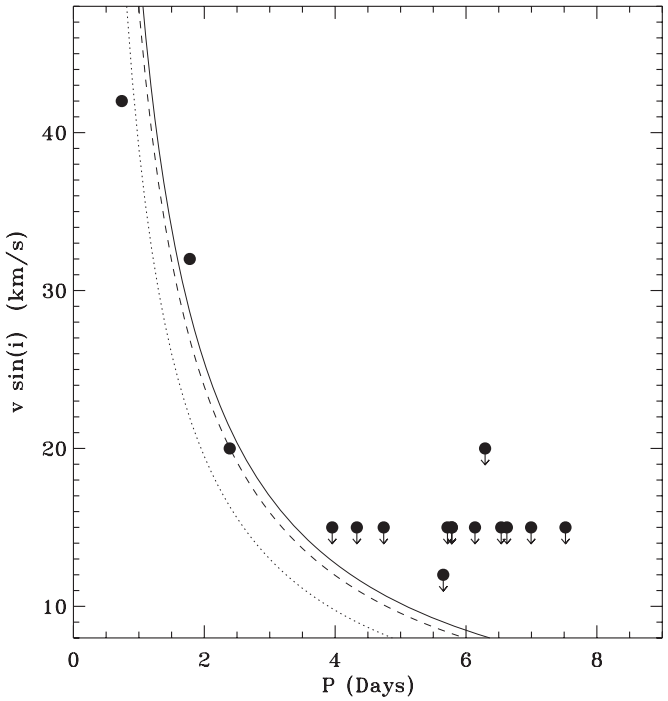

Figure 4. Projected rotation velocities (Barrado y Navascués et al. 2001) plotted against the measured rotation period for 16 stars in M35. All stars have $P_{RV} \geqslant 60\%$ and none of the 16 stars are spectroscopic binaries. For comparison, the solid, dashed, and dotted curves indicate the relation between rotation period and the projected rotational velocity for a solar-like star with a 90°, 70°, and 50° inclination of the rotational axis, respectively. The rotation periods and the projected rotation velocities are consistent for all the 16 stars.

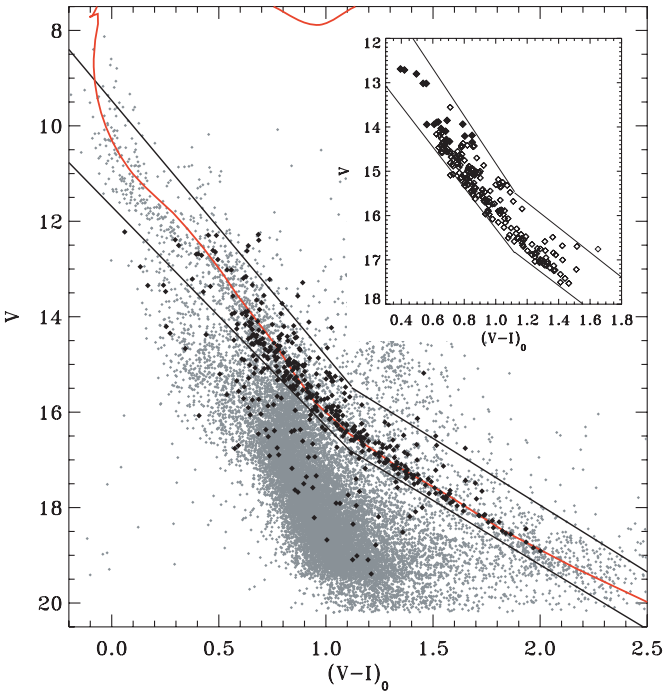

Figure 5. M35 $(V - I)_0$ vs. V CMD. Photometry was provided by C. P. Deliyannis (2008, private communication). The 441 stars with rotation periods are highlighted in black. Stars located between the solid lines are considered photometric members of M35. Note that the faint limits for proper-motion and radial velocity surveys are $V \simeq 14.5$ and $V \simeq 17.5$, respectively. The inset shows the location of stars that are radial velocity members (open symbols), and radial velocity and proper-motion members (filled symbols). These kinematic members of M35 were used to define the boundaries for photometric membership. The isochrone shown represents a 150 Myr Yale model (Yi et al. 2003).

(A color version of this figure is available in the online journal.)

photometric nonmembers). The radial velocity cluster membership probability of each star is calculated using the formalism by Vasilevskis et al. (1958). The mean or center-of-mass radial velocity of a single or binary star was used when calculating the membership probability. We have adopted 50% as the threshold for assigning radial velocity and proper-motion cluster membership. Of the 259 rotators with one or more radial velocity measurement, 203 are radial velocity members of M35 and 20 of those 203 stars are also proper-motion members. More detailed descriptions of the radial velocity survey and membership determination can be found in Meibom & Mathieu (2005), Meibom et al. (2006), and E. Braden et al. (2009, in preparation).

2.5. The M35 Color–Magnitude Diagram and Photometric Membership

Figure 5 shows the $(V-I)$ versus V CMD for M35. The photometry was kindly provided by C. P. Deliyannis (2008, private communication) who obtained *UBVRI* data in a $23' \times 23'$ central field and *BVRI* data in a 2×2 mosaic for a total of $\sim 40' \times 40'$ using the WIYN 0.9 m telescope. In the CMD, the 441 stars for which we have measured rotation periods are highlighted in black. The solid lines enclosing stars within or above the cluster sequence (allowing for inclusion of equal-mass binaries) show our criteria for photometric membership. The inset in Figure 5 shows the location in the M35 CMD of only radial velocity members (open symbols), and radial velocity and proper-motion members (filled symbols), the location of which was used to define the criteria for photometric membership. There are 23 photometric members with three or more radial velocity measurements and a radial velocity membership probability of less than 50%. Those 23 stars were removed from the list of cluster members. The final number of stars with measured rotation periods selected as radial velocity and/or photometric members of M35 is 310.

3. THE ROTATION-PERIOD DISTRIBUTION

The 310 members of M35 with determined rotation periods correspond to ∼12% of the photometric cluster population within the brightness and areal limits of our photometric survey. Figure 6(a) shows the distribution of rotation periods, which spans more than 2 orders of magnitude from ∼0.1 days to ∼15 days. The distribution peaks shortward of 1 day and has a broader and shallower peak centered at about 6 days.

Figure 6(b) displays with an increased resolution of 0.1 day the distribution of rotation periods shortward of 1 day. The dashed and gray histograms, respectively, represent all stars and all cluster members with detected rotation periods. The distribution shows that we are capable of detecting rotation periods down to the pseudo-Nyquist period-limit of about 2 hr (∼0.08 day) resulting from our typical sampling cadence of about 1 hr^{-1} in 2002 December. The distribution of rotation periods for cluster members falls off shortward of 0.3–0.4 days. Two member stars have rotation periods between 0.1 days and 0.2 days, corresponding to surface rotational velocities of 50% or more of their breakup velocities ($v_{br} = \sqrt{(GM_\star/R_\star)}$). We argue based on this inspection of the short-period tail of the distribution that the lower limit of 0.1 days for our period search was set appropriately for the stars in M35.

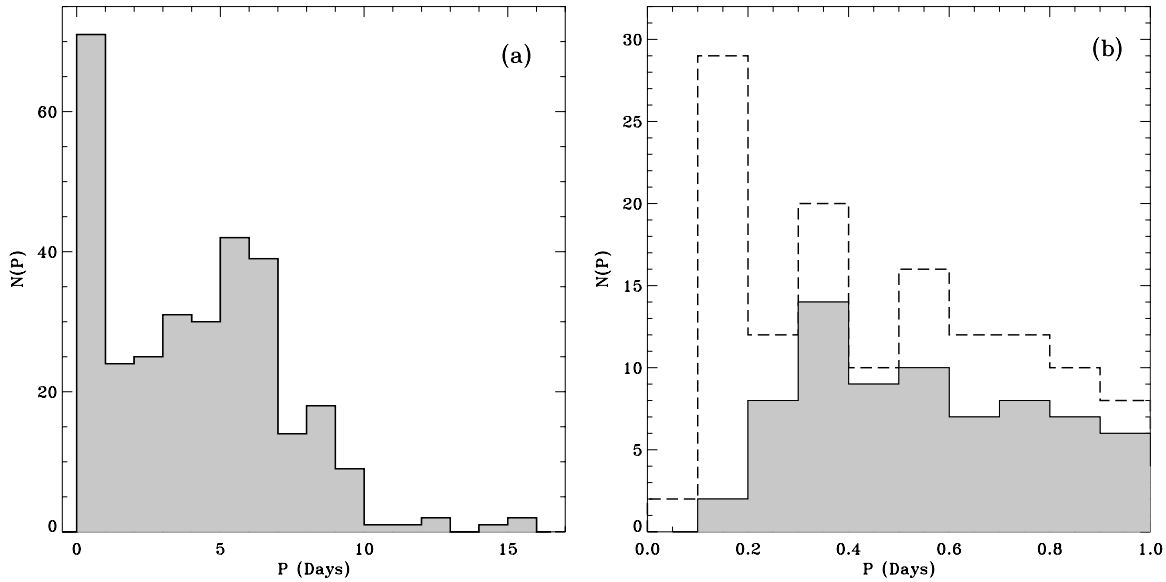

Figure 6. (*a*) Distribution of rotation periods for the sample of 310 cluster members with masses from ∼0.6 to 1.4 $M_{\odot}$ (spectral-type late-K to mid-F). The distribution shows a large dispersion from ∼0.1 days to ∼15 days, and a distinct peak at ⩽1 day and a shallower and broader peak centered at ∼6 days. (*b*) Distribution of rotation periods shortward of 1 day binned in 0.1 day bins. The dashed line histogram represents member as well as nonmember stars with measured rotation periods in our sample. The gray histogram represents only members of M35.

The long-period ends of the period distributions for members and nonmembers (Figure 16, Appendix C) show that the long timespan of the queue-scheduled data enable us to detect rotation periods beyond the ∼10 days typically found to be the upper limit in photometric surveys with durations similar to our short-term 2002 December observing run. We report the detection of 18 stars with rotation periods longer than 10 days, seven of which are members of M35. The longest rotation period among members is 15.3 days, and among the field stars rotation periods of up to ∼17 and 23 days have been measured. In the M35 period distribution, we see a drop-off at ∼10 days. If the ∼12% of the cluster's late-type population with measured rotation periods is a representative sample of the late-type stellar population in M35, then the ∼10 day cutoff may represent a physical upper limit on the rotation-period distribution at 150 Myr. However, it is also possible that we are not capable of detecting the slowest rotators despite our long-baseline photometric survey. Indeed, the modest number of rotation periods longer than 10 days found in the much larger sample of field stars may reflect that the frequency and size of spots on stars rotating slower than ∼10 days is insufficient for detection with the photometric precision of our data. Indeed, X-ray observations in Orion (Stassun et al. 2004) indicate that rotation-period studies of young stars may in general be biased against very slow rotators because such stars likely do not generate strong activity, and thus are not sufficiently spotted to allow detection of photometric periods. Measuring the rotation for such slowly rotating stars will likely require either higher photometric precision or high resolution ($R \gtrsim 50{,}000$) spectroscopic observations to measure projected rotation velocities. The small sample of M35 member stars with periods above 10 days will be discussed in Section 5.5.

3.1. Long-term Stability of the Number, Sizes, and Configurations of Stellar Spots and Spot-groups

We find that for almost all cluster and field stars with measured rotation periods, the long-term queue-scheduled data, spanning ∼5 months in time, phase up with and coincide with the short-term data (16 nights in 2002 December) in the light curves. We tested further the agreement between the short- and long-term photometric variability, by measuring the rotation period separately from the short- and long-term data for 20 randomly chosen stars. For all but one star we found a difference between the two rotation periods that was less than 1% of the period measured from the short-term data alone (in most cases the difference was less than 0.1%). We examined the 20 light curves with all data phased to the period derived from only the short-term data. For all but one star, the long-term data produced light curves of the same shape and phase as the light curves based only on the short-term data. Even for two light curves with clear signs of multiple spots (spot-groups), the short- and long-term data coincided very well. Because it is unlikely that the disappearance and recurrences of spots will result in a light curve with the same shape, amplitude, and phase, the agreement suggests stability of individual spots and/or spot-groups over the ∼5 month timespan of our photometric observations.

We find that the stability of the sizes and configurations of spots on young stars have recently been studied for, e.g., the solar analog PMS star V410 Tau (Stelzer et al. 2003) and for stars in the PMS cluster IC348 (Nordhagen et al. 2006). For V410 Tau data has been collected for over two decades, showing changes in the shape of the light curve over the last decade. The authors suggest that the observed changes reflect variations of the structure of the active regions over timescales of years. However, stability in the rotation period and the recurrence of the light curve minimum, suggest stability of the largest spots over years, and either a lack of latitudinal differential rotation in V410 Tau, or confinement of its spots to a narrow range of latitudes. Similarly, Nordhagen et al. (2006) finds a remarkable stability over seven years in the rotations periods for stars in IC348, suggesting again that these PMS stars do not have significant differential rotation, or that their spots are constrained to a narrow range of stellar latitudes. However, contrary to what is observed over five months in M35, all periodic stars in IC348, as well as V410 Tau, do show changes in the light curve shape and amplitude from year to year.

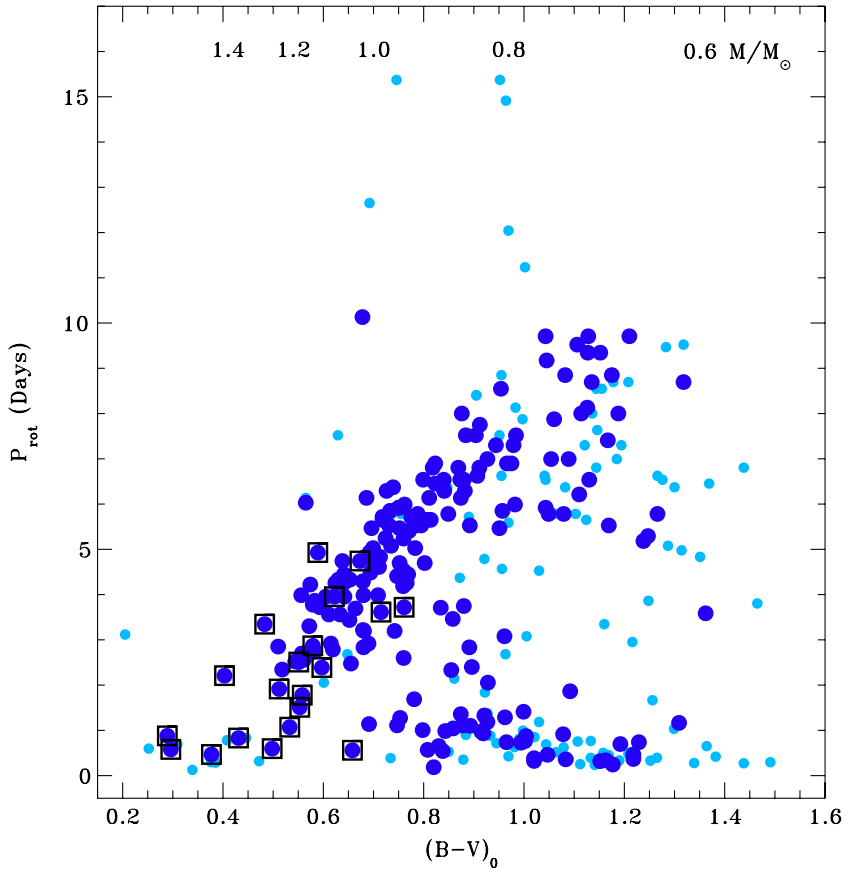

Figure 7. Distribution of stellar rotation periods with $(B-V)$ color index for 310 members of M35. Dark blue (black) symbols represent stars that are both photometric and radial velocity members of M35. Light blue (gray) symbols are used for stars that are photometric members only. Proper-motion members are marked with additional squares. The upper x-axis gives a stellar mass estimate corresponding to the color on the lower axis. Masses are derived using a 150 Myr Yale isochrone.

(A color version of this figure is available in the online journal.)

4. THE M35 COLOR–PERIOD DIAGRAM—THE DEPENDENCE OF STELLAR ROTATION ON MASS

In Figure 7, we display the rotation periods for the 310 members plotted against their $B-V$ color indices, or equivalently their masses. The color indices derive from the deep multiband photometry by C. P. Deliyannis (2008, private communication; Section 2.5) and the corresponding stellar mass estimates (upper x-axis) from a fit of a 150 Myr Yale stellar evolutionary model (Yi et al. 2003) to the M35 CMD. Dark blue symbols represent stars that are both photometric and radial velocity members of M35. Light blue symbols are used for stars that are photometric members only. Proper-motion members are marked with additional squares.

The M35 color–period diagram shows striking structure. The coeval stars fall along two well defined sequences apparently representing two different rotational states. One sequence displays clear dependence between period and color, starting at the blue end at $(B-V)_0 \simeq 0.5$ ($M_\star \simeq 1.2\ M_\odot$) and $P_{\rm rot} \simeq 2$ days and forming a rich diagonal band of stars whose periods are increasing with increasing color index (decreasing mass). This sequence terminates at about $(B-V)_0 \simeq 1.2$ ($M_\star \simeq 0.65\ M_\odot$) and $P_{\rm rot} \simeq 10$ days. The second sequence consists of rapidly rotating ($P_{\rm rot} \lesssim 1$ day) stars and extends from $(B-V)_0 \simeq 0.7$–0.8 ($M_\star \simeq 0.9$–$1.0\ M_\odot$) to $(B-V)_0 \simeq 1.5$ ($M_\star \lesssim 0.5\ M_\odot$). This well-defined sequence of rapidly rotating stars shows a small but steady decrease in rotation period with increasing color (decreasing mass). Finally, a subset of stars are distributed in between the two sequences, and 10 stars have rotation periods that are unusually long, placing them above the diagonal sequence in Figure 7.

The M35 color–period diagram gives a clear picture of preferred stellar rotation periods as a function of color for 150 Myr late-type dwarfs. With the added dimension of color, the diagram take us beyond the one-dimensional period distribution and shows which stars are responsible for the structure observed in Figure 6. The short-period peak at $\lesssim$1 day is due primarily to the rapidly rotating late G and K dwarfs ($M \lesssim 0.9\ M_\odot$), and the sharpness of this peak is the result of little dependence of rotation on color within this group. The more slowly rotating mid-to-late G and K dwarfs give rise to the broader peak at ∼6 days, while the early to mid G dwarfs and some cooler stars fill in the distribution between the peaks.

The two sequences of stars in the color–period diagram represent the most likely/stable rotation period(s) for a given stellar mass at the age of M35. Under the assumption that rotation periods increase with time for all stars, the more sparsely populated area between the two sequences must then represent a phase of rotational evolution of shorter duration. We will discuss the different loci in the color–period diagram in more detail in Section 5.

5. ANGULAR MOMENTUM EVOLUTION AND THE COLOR–PERIOD DIAGRAM

Sequences similar to those observed in the M35 color–period diagram were noted by Barnes (2003, hereafter B03) from careful examination of compilations of rotation-period data from photometric monitoring campaigns on open clusters and field stars. B03 named the diagonal sequence of stars on which rotation periods increase with color the *interface* sequence (or I sequence), and the sequence of rapidly rotating stars the *convective* sequence (or C sequence). In what follows, we will adopt these names for the two sequences in the M35 color–period diagram.

B03 argues that the rapidly rotating stars on the C sequence have radiative cores and convective envelopes that are decoupled. For these stars, he suggests that the evolution of their surface rotation rates is governed primarily by the moments of inertia of the convective envelope and by inefficient wind-driven loss of angular momentum linked to small-scale convective magnetic fields. For stars on the I sequence, large-scale (Sun-like) magnetic fields provided by an interface dynamo couple the core and envelope, and the rotational evolution of the I sequence stars is thus primarily governed by the moments of inertia of the entire star and more efficient angular momentum loss (i.e., a Skumanich 1972 style spin-down). Accordingly, B03 suggests that a late-type star, in which the core and envelope are decoupled as it settles on the ZAMS, will begin its main-sequence life on the C sequence and evolve onto the I sequence when rotational shear between the stellar core and envelope establish a large-scale dynamo field that couples the two zones and provide efficient magnetic wind loss. Higher mass stars have thinner convective envelopes with smaller moments of inertia than low-mass stars and thus leave the C sequence sooner. Stars that are either fully radiative or fully convective will remain as rapid rotators.

Color–period diagrams for coeval populations of different ages allow us to examine the rotational properties of late-type coeval stars as a function of their mass and age, and may bring us closer to understanding the physical mechanisms (internal and/or external) regulating their rotational evolution. The M35 color–period diagram, rich in stars and cleaned for spectroscopic and photometric nonmembers, reveals the morphology described by B03 more clearly than any published stellar populations. We therefore begin with a discussion of the M35 result in the context of the framework developed by B03.

5.1. Timescales for Migration from the C to the I Sequence

In Figure 8, we add M35 to Figure 3 in B03 which shows the relative fractions of stars with $0.5 \leqslant (B-V)_0 \leqslant 1.5$ on the I and C sequences for stellar populations of distinct ages. With rotation periods measured over more than 2 orders of magnitude for confirmed spectroscopic and photometric cluster members, M35 adds the statistically most secure data points to this figure. M35 fit well with the evolutionary trends of increasing relative fractions of C sequence (and gap) stars and decreasing fractions of I sequence stars for younger cluster populations. The almost linear trends in Figure 8 suggest that the decrease and increase in the number of stars on the C and I sequences, respectively, are approximately exponential with time. Under the presumption of an exponential time dependence and that all stars start on the C sequence at the ZAMS, we can estimate the characteristic timescale for the rotational evolution of stars off the C sequence and onto the I sequence, by counting stars on both sequences and

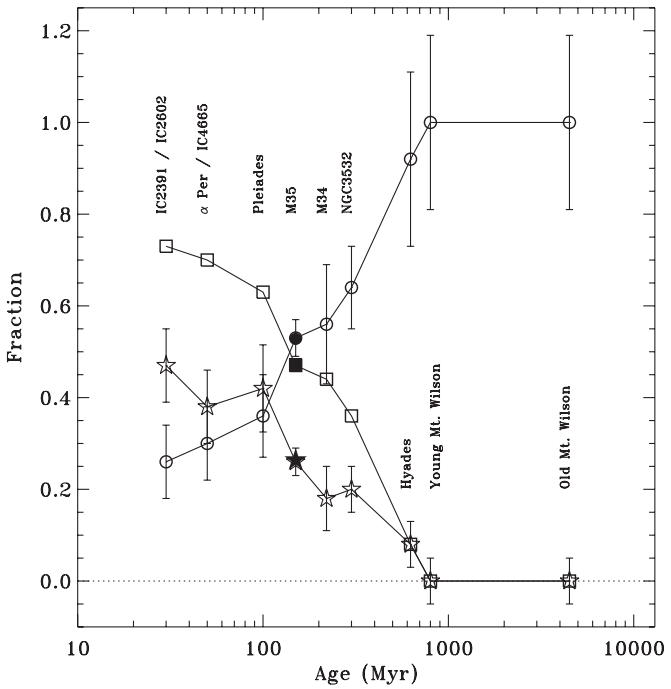

Figure 8. Figure 3 from B03 with M35 added. The figure shows the fractions of stars with $0.5 \leqslant (B-V)_0 \leqslant 1.5$ on the I sequence (circles) and the C sequence (stars) for clusters of different ages. The squares represent the relative fraction of the sum of C sequence and gap stars. The filled symbols show the relative fractions for M35. We follow B03 in estimating the uncertainties in the fractions by the square root of the number of stars.

in the gap in the M35 color–period diagram. Such timescales may offer valuable constraints on the rates of internal and external angular momentum transport and on the evolution rates of stellar dynamos in late-type stars of different masses.

When counting the number of stars on the I and C sequences and in the gap, we use the following criteria. Stars located in the color–period diagram between the lines represented by $P_{\rm rot} = 10(B-V)_0 - 2.5 \pm 2.0$ and with periods above 1.5 days were counted as I sequence stars (see dotted lines in Figure 11). Stars redder than $(B-V)_0 = 0.6$ and with periods between 0 and 1.5 days were counted as C sequence stars. Stars located below $P_{\rm rot} = 10(B-V)_0 - 4.5$ and with periods above 1.5 days were counted as gap stars. These selection criteria are subjective and although the sequences are well defined, the I sequence becomes broader redward of $(B-V)_0 \simeq 1.0$ making the distinction between I sequence and gap stars more difficult. However, due to the large number of rotation periods in M35, the small number of stars that might be moved from the gap to the I sequence or vice versa by using slightly different criteria will not influence the relative fractions and thus the timescales in any significant way.

The number of C sequence stars (N_c) at a time t can then be expressed by

$$N_c = N_{c_0} e^{-t/\tau_c}, \quad (1)$$

where N_{c_0} and τ_c are, respectively, the total number of stars on the I and C sequences and in the gap, and the characteristic exponential timescale. We use the $B-V$ color index to divide the stars into G-dwarfs ($0.6 < B-V < 0.8$) and K dwarfs ($0.8 < B-V < 1.3$) We count all stars within each color-interval in the color–period diagram as N_{c_0}, all C sequence stars within each color-interval as N_c, and adopt 150 Myr as the age of M35. We derive from Equation (1) $\tau_c^G = 60$ Myr and

$\tau_c^K = 140$ Myr as the characteristic exponential timescales for transition between the C and the I sequence for G and K dwarfs, respectively.

We can qualitatively verify these timescales by a comparison between the M35 color–period diagram and those of the younger Pleiades cluster and the older cluster NGC3532 presented in B03. In M35, only seven G dwarfs ($0.6 \lesssim (B-V)_0 \lesssim 0.8$) are found on the C sequence and in the gap, while the G dwarf I sequence is well defined and rich. In contrast, the M35 C sequence and gap are rich in K dwarfs ($0.8 \lesssim (B-V)_0 \lesssim 1.3$), whereas the K dwarf I sequence is less densely populated and less well defined. The lack of G dwarfs on the C sequence seen in M35 is already apparent at 100 Myr in the Pleiades color–period diagram, indicating that the characteristic timescale for G dwarfs to evolve off the C sequence and onto the I sequence is less than ∼100–150 Myr. The rich population of early- and mid-K dwarfs on the M35 C sequence have evolved off the C sequence and onto a well-defined I sequence by the age of NGC 3532 (300 Myr). The NGC 3532 C sequence and gap, however, are populated by late K dwarfs, suggesting that early to mid K dwarfs evolve onto the I sequence on a timescale between 150 and 300 Myr, or approximately twice the time required for G dwarfs. Finally, by the age of the Hyades only three late K or early M dwarfs have been found off the I sequence, or in the gap (see Figure 1 in B03 or Figure 9 below), suggesting that such stars evolve off the C sequence and possibly onto the I sequence on a timescale of ∼600 Myr, or approximately twice the time required for the early to mid K dwarfs.

There is thus good agreement between the exponential timescales derived from the M35 color–period diagram alone and the estimated timescales based on a comparison of color–period diagrams of different ages. We note that a least-squares fit of an exponential function to the C sequence fractions in Figure 8, gives a timescale of 106 Myr for a decrease in the number of C sequence stars by a factor of e.

5.2. Testing the Skumanich $\sqrt{t}$ Spin-Down Rate Between M35 and the Hyades

The color–period diagram for the Hyades contains 25 stars (Radick et al. 1987; Prosser et al. 1995), 22 of which form an I sequence of G and K dwarfs. Despite the smaller number of stars, the blue part of the Hyades I sequence, populated by G dwarfs, is well defined. By comparing the rotation periods for the I sequence G dwarfs in M35 to those of the I sequence G dwarfs in the ∼4 times older Hyades, we can directly test the Skumanich (1972) $\sqrt{t}$ time dependence on the rotation-period evolution for stars in this mass range. We follow B03 in assuming separate mass and time dependences for stellar rotation, and that the same mass dependence can be applied to different stellar populations. Adopting an age of 625 Myr for the Hyades (Perryman et al. 1998) and of 150 Myr for M35, we decrease the Hyades rotation periods by $\sqrt{625/150} \simeq 2$. We show in Figure 9 the color–period diagram with the 310 M35 members (all gray symbols) and with the locations of the 25 Hyades stars overplotted (black symbols). The spun-up Hyades I sequence G dwarfs coincide nicely with the M35 I sequence G dwarfs, in support of the Skumanich $\sqrt{t}$ time dependence for such stars. Curiously, the Hyades K dwarfs, also spun-up according to the Skumanich law, have rotation periods systematically shorter than the M35 K dwarfs. At face value, this suggests that the time dependence for spin-down of K dwarfs is different and slower than for G dwarfs between 150 Myr and 625 Myr.

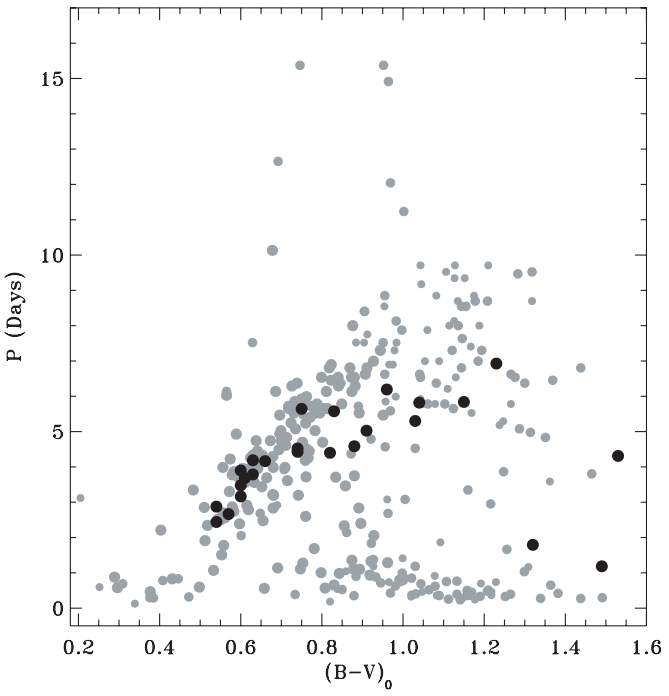

Figure 9. M35 color–period diagram (gray symbols) with 25 Hyades stars overplotted (black; Radick et al. 1987; Prosser et al. 1995). All but the three reddest Hyades stars fall on a sequence similar to the M35 I sequence. All Hyades rotation periods were spun-up by a factor of $\sqrt{625/150} \simeq 2$ in accordance with the Skumanich $\sqrt{t}$ time dependence on stellar rotation evolution, assuming ages of 625 Myr and 150 Myr for the Hyades and M35, respectively.

5.3. The Gyro-age of M35

Arguing that the rotation of stars on the C and I sequences follow separate mass (M) and age (t) dependences ($P(t, M) = g(t) \times f(M)$), B03 introduced heuristic functional forms to represent these separate dependences of the I and C sequences. Barnes (2007, hereafter B07) presents a modified functional form for the I sequence. These functions define one-parameter families, with that parameter being the age of the stellar population, and the resulting curves in the color–period plane represent a set of rotational isochrones. We note that B03 use $g(t) = \sqrt{t}$ (Skumanich), while B07 derive $g(t) = t^{0.52}$ by requiring that a solar-like star spin down to solar rotation at solar age.

Kawaler (1989) used his own calibrated angular momentum loss law (Kawaler 1988) and the assumption of solid body rotation after ∼100 Myr (Pinsonneault et al. 1989), to derive a relationship between stellar age, rotation period, and color. Kawaler's age–period–color relation is thus based on models calibrated to the Sun, and the assumption that the Skumanich relationship is valid for all masses. He express the stellar mass, radius, and moment of inertia, in terms of observables such as stellar color, via stellar models.

We note that our result in Section 5.2 suggest that the time dependence of stellar rotation is not independent of stellar mass, as assumed by both B03, B07, and Kawaler (1989).

The well defined sequences in the M35 color–period diagram make possible a test of the period–color relations proposed by B03, B07, and Kawaler (1989). We show in Figure 10 the M35 color–period diagram with the B03 and B07 rotational isochrones for the independently determined stellar-evolution age for M35 of 150 Myr (von Hippel et al. 2002; C. P. Deliyannis 2008, private communication). The rotational isochrones match

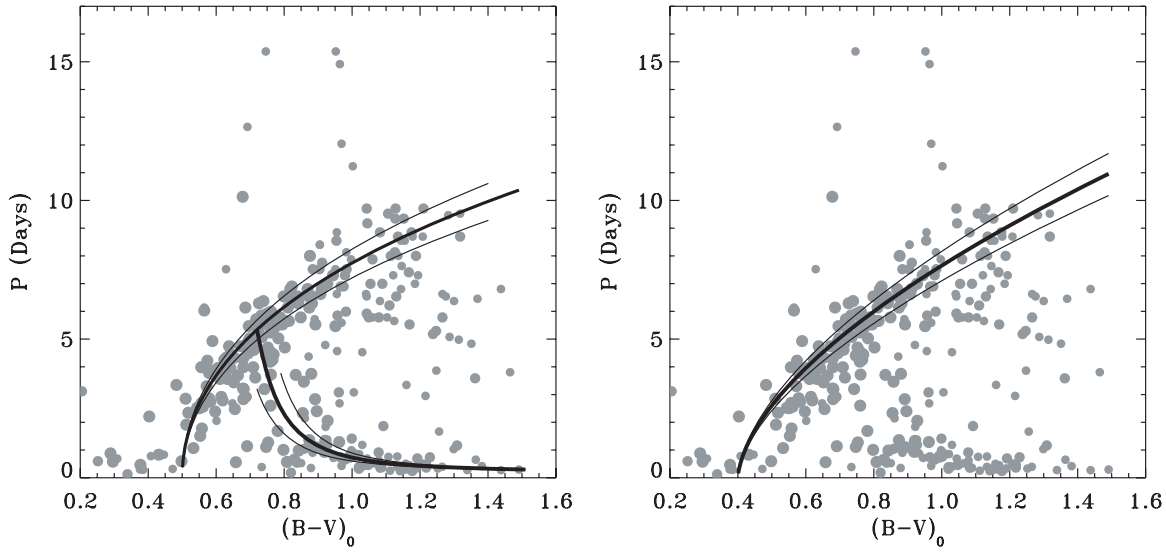

Figure 10. M35 color–period diagram with the 150 Myr rotational isochrones from B03 (left) and B07 (right) overplotted as a thick black solid curves. To illustrate the sensitivity to age, we show the 130 Myr and the 170 Myr isochrones as thinner curves flanking the 150 Myr isochrones.

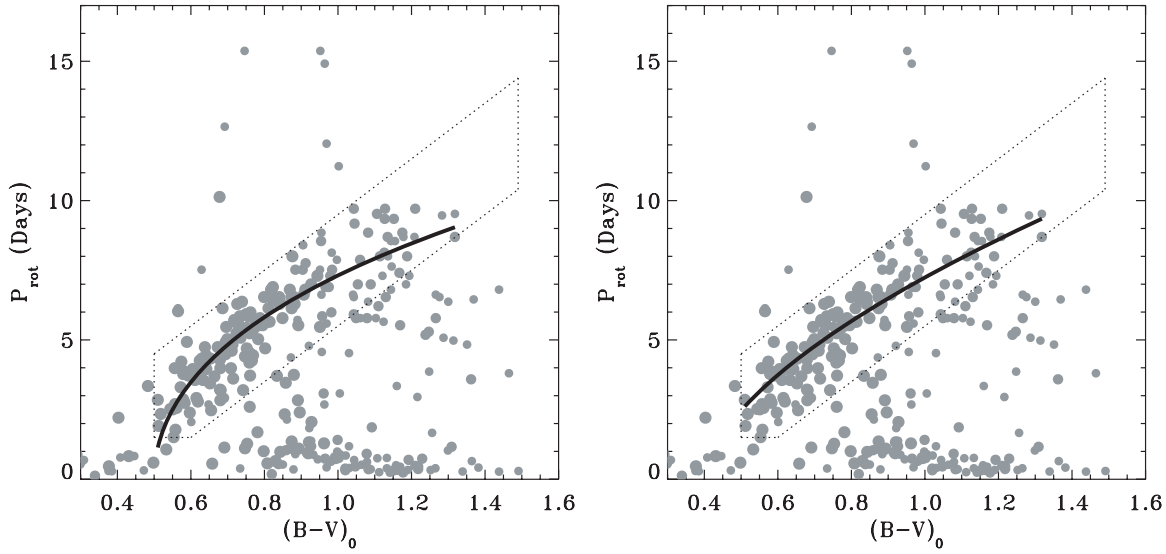

Figure 11. Least-squares fit of the B03 I sequence isochrone (left; Equation (2)) and the B07 I sequence isochrone (right; Equation (3)) to the M35 I sequence with age (t) as a free parameter. The gyro-ages corresponding to the fits are 133.9 ± 3 Myr and 133.5 ± 3 Myr, respectively. The I sequence stars to which the isochrones were fitted are enclosed by the dotted lines in both figures.

the M35 I and C sequences well, suggesting that they can indeed provide a consistent age estimate (gyro-age) for a cluster based on a well populated color–period diagram cleaned for nonmembers. To illustrate the sensitivity to age, rotational isochrones for 130 Myr and 170 Myr are also displayed in Figure 10.

Assuming no prior knowledge about the age of M35 (thus letting age be a free parameter), we perform a nonlinear least-squares fit to the I sequence stars (enclosed by the dotted lines in Figure 11) of the functional form of the rotational I sequence isochrones from B03:

$$P(t,(B-V)) = \sqrt{t}\times(\sqrt{((B-V)-a)}-b((B-V)-a) \quad (2)$$

with $a = 0.50$, and $b = 0.15$, and from B07:

$$P(t,(B-V)) = t^{0.52} \times (c((B-V)-d)^{f}) \quad (3)$$

with $c = 0.77$, $d = 0.40$, and $f = 0.60$.

When fitting, the I sequence stars were weighted them according to their cluster membership, with most weight given to confirmed radial velocity and proper-motion members and least weight given to stars with only photometric membership. The weights given to individual stars are listed in Table 2 in Appendix B. Figure 11 shows the best fits of both Equations (2) and (3) to the M35 I sequence. The derived age is 134 Myr for both functional forms, each with a formal 1σ uncertainty of $\sim$3 Myr. The close agreement of the two ages likely reflects the similar shape of the two isochrones over the color interval from $\sim$0.5 to 1.0 where the M35 I sequence is most densely populated. The small formal uncertainties reflect a well-defined I sequence rich in stars. However, the gyro-ages may still be affected by systematic errors in the stellar evolutionary ages for the young open clusters.

Alternatively, we show in Figure 12 the distribution of gyro-ages of the M35 I sequence stars, calculated using the age–period–color relations of B03 (left panel) and B07 (right panel).

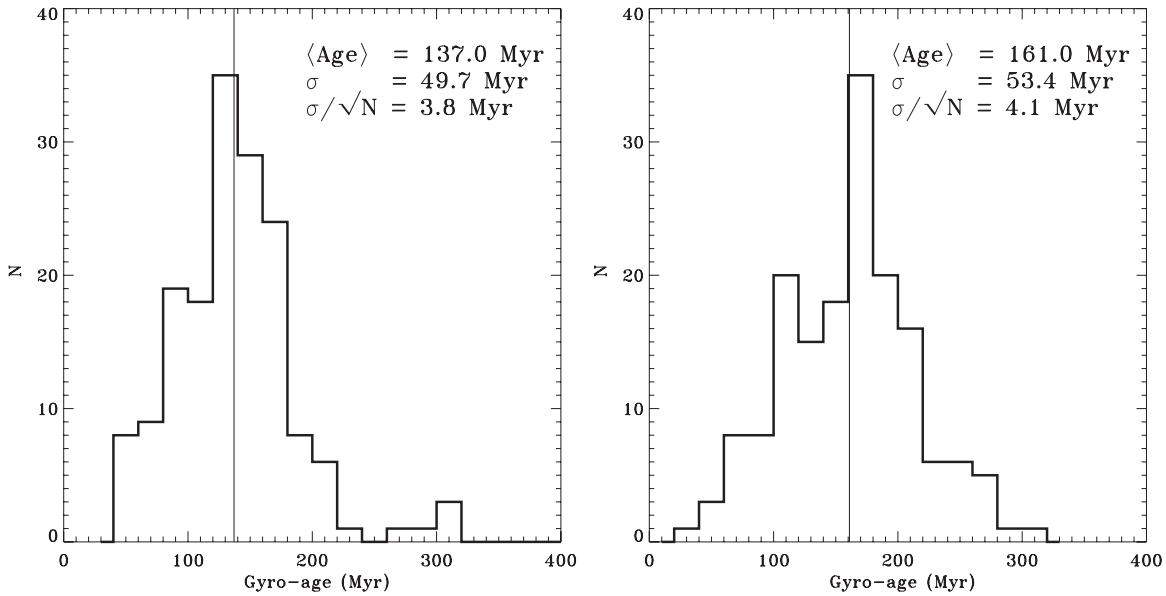

Figure 12. Distribution of gyro-ages for M35 I sequence stars. The panels show the distributions of M35 gyro-ages calculated using the B03 (left panel) and B07 (right panel) age–rotation–color relations. The distribution mean, standard deviation, and standard error on the mean, are given in the upper right corner of each panel.

The mean gyro-ages of 137 Myr and 161 Myr, are both close to the 150 Myr derived for the cluster using the isochrone method (see Section 1). Assuming that all I sequence stars are truly coeval, the standard errors of 3.8 Myr and 4.1 Myr give uncertainties on the calculated mean gyro-ages for M35 of 2.8% and 2.5%, close to the formal uncertainty on the least-squares fits. The close agreement between the mean gyro-age (137 Myr) and the gyro-age determined from the least-square fit (134 Myr), as well as a smaller standard deviation in the gyro-age distribution, suggest that the B03 I sequence isochrone (Equation (2)) provide a better match to the color dependence of stellar rotation on the I sequence than the B07 isochrone (Equation (3)).

In Figure 13, we show the corresponding distribution of gyro-ages calculated using the Kawaler (1989) age–period–color relation. The mean age is equal to that derived for the B07 relation, while the larger σ and standard error (3.3%) reflects primarily a poorer fit to the M35 I sequence for the late F and early G-type stars, resulting in gyro-ages that are too low for those stars.

5.4. Improving the I Sequence Mass–Rotation Relation Using M35

The method of gyrochronology relies on fitting the I sequence rotational isochrone, with age as a free parameter, to populations of cluster stars or to individual field stars in the color–period plane B07. The functional dependence between stellar color and rotation period of the isochrone will thus directly affect the derived gyro-age, and will, if not accurately determined, introduce a systematic error. It is therefore important to constrain and test the mass–rotation relation for stars on the I sequence as new data of sufficiently high quality becomes available.

Our data for M35 are well suited for such a test because of the rich and well defined I sequence, the extensive knowledge about cluster membership, and the independent stellar evolution age for the cluster. To constrain the color–period relation, we fit Equations (2) and (3) to the M35 I sequence, using the same selection of stars and the same fitting weights as described in Section 5.3. We determine all coefficients in Equations (2) and (3) for the fixed cluster age (t) of 150 Myr. The coefficients with 1σ uncertainties are listed in Table 1 and the corresponding rotational isochrones are shown in Figure 14. To illustrate how closely the isochrones trace the selected I sequence stars, Figure 14 also displays a dashed curve representing the moving average of the rotation periods along the I sequence.

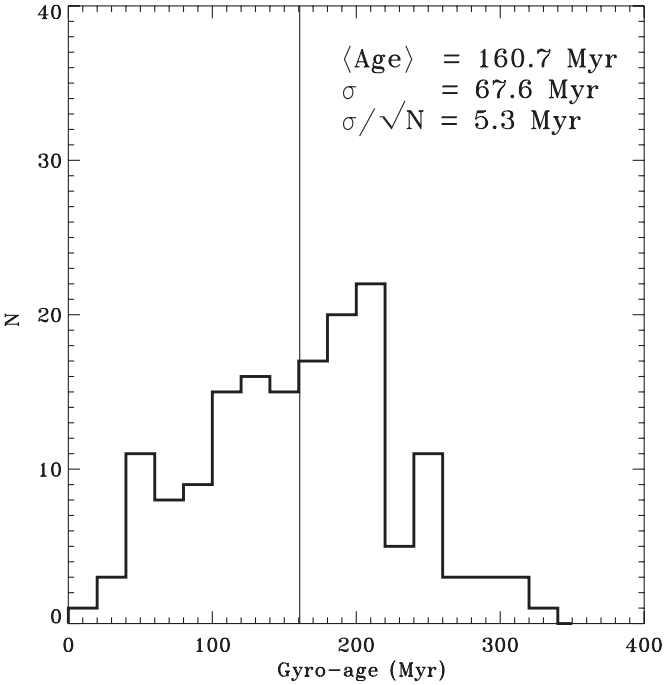

Figure 13. Distribution of gyro-ages for M35 I sequence stars calculated using the Kawaler (1989) age–rotation–color relation. The distribution mean, standard deviation, and standard error on the mean, are given in the upper right corner of each panel.

We can compare the coefficients derived using the M35 data to those chosen and/or derived by B03 and B07. Our best fit of the B03 isochrone confirms the value of 0.5 for the a coefficient chosen (not fitted) by B03 to best represent the color–period data included in his study. a is a translational term that determines

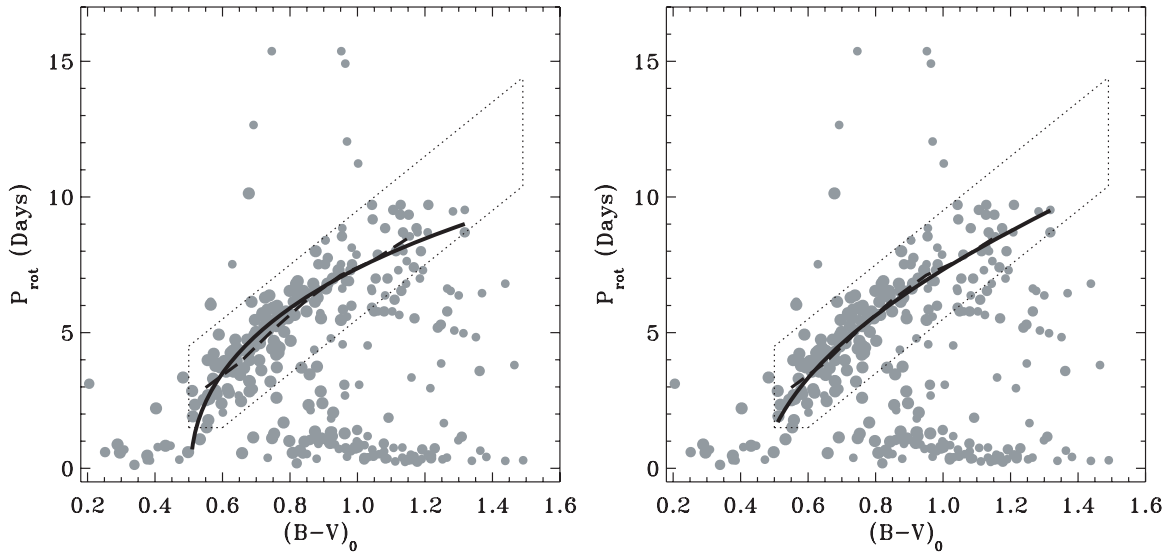

Figure 14. Least-squares fits (solid curves) of 150 Myr B03 (left) and B07 (right) I sequence isochrones (Equations (2) and (3)) to the M35 I sequence. The corresponding new values for the isochrone coefficients *a*, *b*, *c*, *d*, and *f* were determined from the fits and are listed in Table 1. The moving average of the rotation periods for the I sequence stars is also shown as a dashed curve for comparison.

the color for which the isochrone gives a period of 0 days. For the *b* coefficient, our best fit give a value of 0.20 compared to the choice of 0.15 by B03. Our larger value of the *b* coefficient results in an isochrone with slightly more curvature.

From our best fit of the B07 rotational isochrone to the M35 I sequence, we determined a *c* coefficient of 0.77, equal to the value used by B07, while our value 0.55 for the *f* coefficient is smaller than the value of 0.60 used by B07. In the case of the *c* and *f* coefficients, B07 also determined their values from least-squares fitting to the I sequence stars of several young open clusters. However, for the translational term *d*, B07 chose a fixed value of 0.4 to allow for more blue stars to be fitted. We left the *d* coefficient as a free parameter when fitting to the M35 I sequence, and got a value of 0.47.

The new value of 0.47 for *d* is particularly interesting as it corresponds to the approximate $B - V$ color for F-type stars at the transition from a radiative to a convective envelope. This transition was noted from observations of stellar rotation (known as the break in the Kraft curve, Kraft 1967), and is associated with the onset of effective magnetic wind breaking (e.g., Schatzman 1962). The value of 0.47 for the *d* coefficient therefore suggest that, for M35, the blue (high-mass) end of the I sequence begins at the break in the Kraft curve.

5.5. Prediction: Tidal Evolution is Responsible for the Unusually Slow Rotators

Ten stars fall above the M35 I sequence, and thus rotate unusually slowly in comparison to other members of M35 with similar masses. All 10 stars are photometric members of M35 and two are also spectroscopic members. We have no reason to believe that the rotation periods for these stars are due to aliases in the power spectra, and we note that a similar pattern is seen in NGC 3532 with seven stars located above the I sequence B03 and in M34 with six stars above the I sequence (S. Meibom et al. 2009, in preparation).

What causes the rotational evolution of these stars to deviate significantly from that of most similar color stars in M35? We propose here that tidal interactions with a close stellar companion has acted to partially or fully synchronize the stellar spins of these stars to the orbital motions, and that such tidal synchronization is responsible for their slower than expected rotation. We thus predict that these 10 stars are the primary stars in binaries with periods of ∼10–15 days.

This proposition finds support from the star of M35 located in the color–period diagram at $(B - V)_0 = 0.68$ and $P_{\rm rot} = 10.13$ days. This star is the primary in a circular binary with an orbital period of 10.33 days. The rotation of this star has been synchronized to the orbital motion of the companion (Meibom et al. 2006), forcing it to rotate more slowly than stars of similar mass. In addition to the spectroscopic binary, three of the remaining nine slow rotators are photometric binaries. Spectroscopic observations has begun of those stars and of the remaining five stars as of 2007 fall to determine their status as binary or single stars, and in the case of binarity, the degree of tidal evolution.

5.6. Stellar Angular Momentum Evolution Near the ZAMS

The trend in Figure 8 of an increasing fraction of C sequence (and gap) stars for younger cluster populations leads naturally to the suggestion that most, if not all, late-type stars pass through a phase of rapid rotation (the C sequence) at the ZAMS. We note that even should this be the case, an *observed* C sequence fraction of 1 is not expected for even the youngest coeval populations, as stars of different masses will reach the ZAMS, and thus hypothetically the C sequence, at different times. For example, late F stars will be the first to arrive at/on the ZAMS and C sequence, and leave it before the arrival of the G- and K-type stars.

The color–period diagrams for the youngest stellar populations presented in Figure 8 (see also Figure 1 in B03) show that most stars lay either on the C sequence or in the gap. B03 finds only 25% of the stars at 30 Myr to be on the I sequence. In fact, the I sequence is not clearly identifiable at this age, and the stars identified as being on the I sequence are early-type rapid rotators near the intersection of the two sequences.

By 30 Myr very few of the cluster members have rotation periods longer than 5 days. This is in marked contrast to fractions

of ∼60% and ∼40%, respectively, for such slow rotators in the PMS populations of the Orion Nebula cluster (ONC) and NGC 2264 (see Herbst et al. 2007). The difference in the numbers of slowly rotating stars pre- and post-ZAMS, suggests that most, if not all, of the stars rotating slowly at ∼1–3 Myr, spin up as they evolve onto the ZAMS. Such spin-up may have been observed. Comparison of the rotation-period distributions for stars in the ∼1 Myr ONC and the ∼2–3 Myr NGC 2264 (Herbst et al. 2007, and references therein) shows a spin-up with time by a factor ∼2, presumably due to conservation of angular momentum as the stars contract on the PMS. On the other hand, the distribution of a smaller sample of rotation periods in the ∼2–3 Myr IC 348 (Nordhagen et al. 2006) does not show similar evidence for spin-up when compared to the ONC.

From the point of view of modeling stellar angular momentum evolution, we emphasize the narrowness of the C sequence, with all rotation periods between 0.5 days and 1.5 days. We suggest that the broad distribution of rotation period among solar-like stars in the PMS populations must collapse into a narrow C sequence of similar rotation periods independent of the mass. Indeed, we suggest that in the two 30 Myr clusters of B03 (Figure 1), the gap stars with $(B-V)_0 \gtrsim 0.9$ may in fact be evolving *toward* the C sequence, and point out that in the 50 Myr clusters in B03, mostly C sequence stars are observed redward of $(B-V)_0 \simeq 0.9$.

6. SUMMARY AND CONCLUSIONS

We present the results of an extensive time-series photometric survey over ∼5 months of late-type members in the 150 Myr open cluster M35 (NGC 2168). We have obtained photometric light curves for 14,022 stars with $12 \lesssim V \lesssim 19.5$ over a $40' \times 40'$ field centered on M35. We have determined the rotation periods for 441 stars. Cluster membership and binarity for stars with rotation periods are determined from the results of a decade long spectroscopic survey in M35. Of the 441 rotators, 310 stars are radial velocity and/or photometric members of M35.

With an age slightly larger than the Pleiades but with a much larger population of late-type stars, M35 is particularly interesting for studying stellar rotational evolution during this active phase of angular momentum evolution between the ZAMS and the age of the Hyades. The rotation periods of the 310 late-type members span over 2 orders of magnitude from 0.1 day (≳50% of their breakup velocities), up to ∼15 days. A drop-off in the period distribution is found at ∼10 days, well below the upper limit of our period search. The ∼10 day cutoff may represent a physical upper limit on the rotation-period distribution at 150 Myr. However, it is also possible that detecting more slowly rotating stars in M35 will require higher photometric precision or higher resolution spectroscopic observations.

We find in the phased light curves for almost all stars with measured rotation periods that the long-baseline (∼5 months), low-frequency (1/night) photometric measurements match the short-baseline (16 nights), high-frequency ($\sim 1\ \mathrm{hr}^{-1}$) measurements in both phase, shape, and amplitude. Further tests on a subset of stars show that the same rotation periods are derived from the short- and long-term data to within 1%. This stability in the modulation of the stellar brightness suggests a similar stability in the configuration, size, and number of starspots.

In the color–period plane, the 310 M35 rotators reveal striking dependences between the surface rotation period and stellar color (mass). More than 75% of the stars lay along two distinct sequences in the color–period diagram, apparently representing two different states in their rotational evolution. Similar sequences were identified by Barnes (2003) for stars in other clusters. Comparison between M35 and these clusters of the locations of the sequences in color–period diagram, as well as the relative numbers of stars on each, support for the idea (proposed by Barnes 2003) that stars evolve from one sequence (C) to the other sequence (I) at a rate that is inversely related to the stellar mass.

We determine from the M35 color–period diagram that the characteristic exponential timescale for rotational evolution off the C sequence and onto the I sequence is ∼60 Myr and ∼140 Myr for G and K dwarfs, respectively. These timescales may offer valuable constraints on the rates of internal and external angular momentum transport and on the evolution rates of stellar dynamos in late-type stars of different masses.

From the emerging trend (supported by M35) of an increasing relative fraction of rapidly rotating C sequence stars with decreasing population age, we propose the hypothesis that most, if not all, late-type stars pass through a phase of rapid rotation (C sequence) on the ZAMS. By conjecture, there may not be a need for a direct connection between slowly rotating stars observed in the early PMS and slowly rotating stars at ∼100 Myr post the ZAMS. Such a connection has often been assumed and set as a constraint on models of stellar angular momentum evolution, motivating the introduction of mechanisms to prevent slowly rotating PMS stars from spinning up as they evolve onto the main sequence.

By comparison with measured rotation periods in the Hyades, we put to the test the empirical Skumanich $\sqrt{t}$ time dependence on the stellar rotation period for G dwarfs. By reducing the Hyades rotation periods by a factor of $\sqrt{\mathrm{Age}_{\mathrm{Hyades}}/\mathrm{Age}_{\mathrm{M35}}}$, we find that the $\sqrt{t}$ law accounts very well for the rotational evolution of G dwarfs between M35 and the Hyades, whereas among the K dwarfs the $\sqrt{t}$ time dependence predicts a spin-down rate that is faster than observed between M35 and the Hyades.

We find that the heuristic rotational isochrones proposed by Barnes (2003) and Barnes (2007) match the location of M35 I and C sequences using the independently determined stellar evolution isochrone age for M35. A nonlinear least-squares fit of the rotational isochrones to the M35 I sequence sets the cluster's gyro-age to 134 Myr with a formal 1σ uncertainty of 3 Myr. We use the age–period–color relations by Barnes (2003), Barnes (2007), and Kawaler (1989), to calculate the distributions of gyro-ages for the M35 I sequence stars. The mean gyro-ages have standard errors of order 3% and agree well with the ∼150 Myr age derived for the cluster using the isochrone method. These results suggest that a well-populated color–period diagram, cleaned for nonmembers, in combination with rotational isochrones, can provide a precise age estimate that is consistent with the age derived from isochrone fitting in the CMD. We also use the M35 I sequence to improve the coefficients for the color dependence of the rotational isochrones.

Finally, to explain the 10 M35 stars rotating with rates that are unusually slow compared to similar stars in the cluster, we propose that tidal synchronization in binary stars with orbital periods of order 10–15 days is responsible. Two of the 10 stars have already been found to be primary stars in tidally evolved spectroscopic binaries, while three stars are photometric binaries. Accordingly, we predict that the remaining stars are

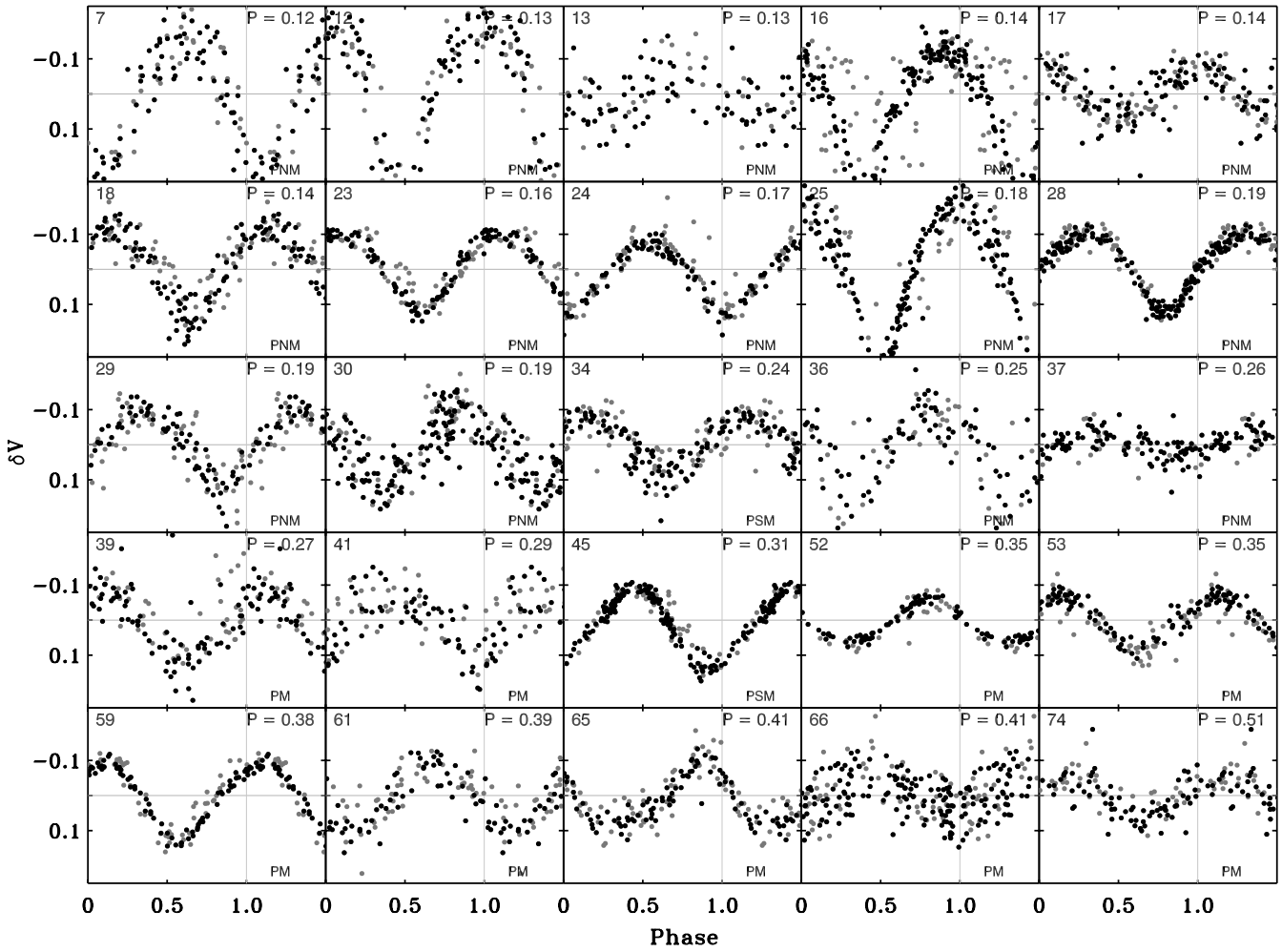

Figure 15. Phased light curves for stars with measured rotation periods. This figure is intended to show examples of our light curves and light curve plots. Phased light curves for all 441 stars can be found in the electronic edition of the journal.

(An extended version of this figure is available in the online journal.)

also primary stars in spectroscopic binaries with orbital periods of ∼10–15 days.

We thank the University of Wisconsin-Madison Astronomy Department and NOAO for the time granted on the WIYN 0.9 m and 3.5 m telescopes. We express our appreciation to the site managers and support staff at both telescopes for their exceptional and friendly support. We are thankful to all observers in the WIYN 0.9 m consortium who provided us with high-quality data through the queue-scheduled observing program. This work has been supported by NSF grant AST-0406615 to the UW-Madison, a PhD fellowship from the Danish Research Academy to S.M., partial support to S.M. from the Kepler mission via NASA Cooperative Agreement NCC2-1390, and by the Cottrell Scholarship from the Research Corporation to K.G.S.

APPENDIX A

PHASED LIGHT CURVES

This appendix presents the light curves for the stars in the field of M35 for which we measured rotation periods. In the printed journal, Figure 15 below show examples of our light curves and light curve plots. Phased light curves for all 441 stars can be found in the electronic edition of the journal. The light curves have been divided into three groups according to the amplitude of the photometric variation. For each group, the light curves are sorted by the rotation period and are presented with the same δV range on the ordinate. The group of stars with the largest photometric variability are shown first.

For each star, we plot the data from the high-frequency survey (2002 December) as black symbols, and data from the low-frequency survey (2002 October through 2003 March) as gray symbols. A running ID number corresponding to the ID number in Table 1 Appendix B is given in the upper left-hand corner in each plot. The period to which the data are phased (the rotation period listed in Table 1 as $P_{\rm rot}$) is given in the upper right corner. The 2–5-letter code in the lower right corner informs about the stars membership status. The codes have the following meaning: photometric member (PM; described in Section 2.5), photometric nonmember (PNM), photometric and spectroscopic member (PSM), photometric and proper-motion member (PPM), and photometric member but spectroscopic nonmember (PMSNM). For each star a horizontal gray line in each plot mark $\delta V = 0.0$ and a vertical gray line marks a phase of 1.0.

Table 1
New Coefficients for the I Sequence Rotational Isochrones

Isochrone	Coefficient	Value	1σ Error
B03	a	0.507	0.005
B03	b	0.204	0.013
B07	c	0.770	0.014
B07	d	0.472	0.027
B07	f	0.553	0.052

APPENDIX B

DATA FOR THE 441 STARS WITH MEASURED ROTATION PERIODS IN THE FIELD OF M35

Table 2 presents the results from this study together with information relevant to this paper for 441 stars in the field of M35. In the printed journal, a stub version of Table 2 shows the form of the full table and a sample of the first five lines of its contents. The full version of the table can be found online. The stars appear in order of increasing rotation period, and the running number in the first column corresponds to the number in the upper left-hand corner of the stars light curve in Appendix A. Columns 2 and 3 give the stellar equatorial coordinates (equinox 2000). Column 4 lists the measured stellar rotation period in decimal days. Columns 5, 6, and 7 give the stellar V magnitude and $B - V$ and $V - I$ color indices, respectively, corrected for extinction and reddening. Column 8 presents the number of radial velocity measurements for the star, and columns 9 and 10 give the mean radial velocity and the velocity standard deviation, respectively. Column 11 lists the radial velocity cluster membership probability calculated using the formalism by Vasilevskis et al. (1958). Column 12 contains a proper-motion cluster membership probability from either Cudworth (1971) or McNamara & Sekiguchi (1986). In Column 13, we give the abbreviated membership codes (initialisms) also found in the light curves in Appendix A. The codes denote the type of membership information available for the star and have the following meaning: photometric member (PM; described in Section 2.5), photometric nonmember (PNM), photometric and spectroscopic member (PSM), photometric and proper-motion member (PPM), and photometric member but spectroscopic nonmember (PMSNM). In Column 14, we give the weights used for each star when fitting the rotational isochrones in Sections 5.3 and 5.4. Finally, in Column 15, the rotational state of the star is indicated by a one-letter code representing, respectively, the I sequence (i), the C sequence (c), and the gap (g). Stars with a "–" in column 15 have locations in the color–period diagram that do not correspond to either of the sequences or the gap.

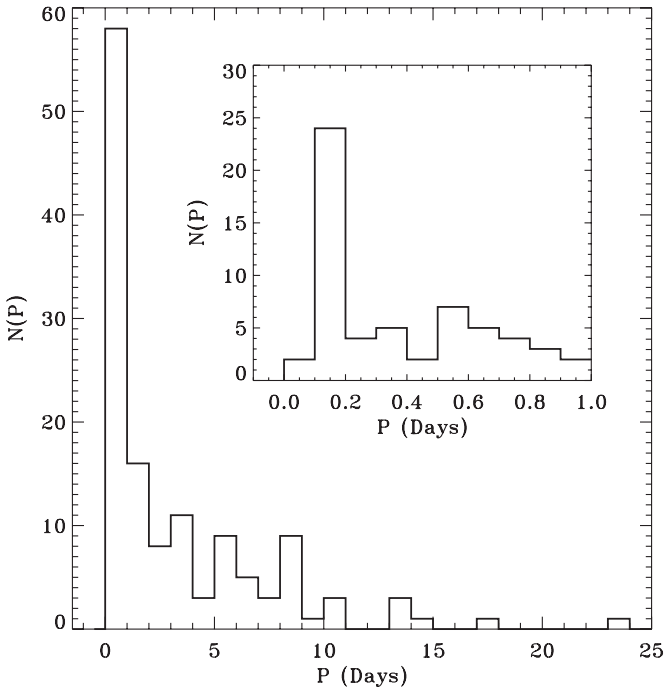

Figure 16. Rotation-period distribution of the 131 radial velocity and/or photometric nonmembers. The inset shows the distribution of periods less than 1 day with an increased resolution of 0.1 day.

APPENDIX C

THE ROTATION-PERIOD DISTRIBUTION OF NONMEMBERS

In this appendix, we display and briefly comment upon the rotation period distribution of the nonmembers among the 441 rotators, which presumably are mostly field stars belonging to the Galactic disk. Unlike the cluster members we do not know the ages, distances, or masses of these stars. We will therefore only comment on a comparison between the two distributions and on distinct features in the period distribution of the 131 nonmembers shown in Figure 16. First, rotation periods are detected over approximately the same range (∼0.1–15 days) as for the 150 Myr cluster members, with only a few stars rotating slower. Second, there appears to be no indication of a bimodal distribution, but rather a distribution with a peak of

Table 2
Data for the 441 Stars with Measured Rotation Periods in the Field of M35

No.[a]	R.A. (h m s)	Decl. (° ′ ″)	P_{rot} (days)	V_0	$(B-V)_0$	$(V-I)_0$	N_{RV}	$\bar{RV}$ (km s^{-1})	σ_{RV} (km s^{-1})	P_{RV} (%)	P_{PM} (%)	mcode[b]	Weight	Sequence[c]
1	6 08 27.136	24 21 16.131	0.088	15.20	0.42	0.50	···	···	···	···	0	PNM	0.0	···
2	6 08 32.183	24 15 33.227	0.096	15.01	0.47	0.64	···	···	···	···	0	PNM	0.0	···
3	6 08 43.198	24 30 01.147	0.107	15.90	0.45	0.64	···	···	···	···	0	PNM	0.0	···
4	6 08 43.282	24 37 24.589	0.112	14.89	0.45	0.61	···	···	···	···	0	PNM	0.0	···
5	6 10 18.959	24 03 17.857	0.126	16.74	0.73	1.05	···	···	···	···	0	PNM	0.0	c

Notes.
[a] Running number assigned to 310 rotators after sorting by rotation period.
[b] Letter code denoting a star's cluster membership status (see the introductory text of the appendix for code meaning).
[c] Letters "i," "c," and "g" mark stars on the I and C sequences or in the gap, respectively.
(This table is available in its entirety in a machine-readable form in the online journal. A portion is shown here for guidance regarding its form and content.)

ultrafast rotators and a long tail of periods up to and beyond 15 days. Third, and most strikingly, as shown by the 0.1 day resolution of the inset in Figure 16, the nonmember distribution exhibits a very distinct peak between 0.1 and 0.2 days. The phased light curves for these stars (Appendix A) show that the majority of these stars have large and well defined photometric variability with peak-to-peak amplitudes of $0\overset{m}{.}1$ or higher. It is possible that most of these stars are contact binaries of, e.g., the W UMa-type. Such systems typically have orbital periods of order 0.2–0.5 days and occur with a frequency of ∼0.2% (OGLE Variable Star Catalog; Rucinski 1997). The frequency of rapidly varying nonmembers found in the field of M35 is ∼20 out of 13,700 or ∼0.15% and thus in good agreement with that found from the OGLE Catalog. Indeed, if the light curves for these stars represent eclipses rather than spot-modulation, then the measured periods must be doubled bringing them into the expected range for W Uma systems.

REFERENCES

Alphenaar, P., & van Leeuwen, F. 1981, Inf. Bull. Var. Stars, 1957, 1
Barnes, S. A. 2003, ApJ, 586, 464
Barnes, S. A. 2007, ApJ, 669, 1167
Barnes, S., & Sofia, S. 1996, ApJ, 462, 746
Barrado y Navascués, D., Deliyannis, C. P., & Stauffer, J. R. 2001, ApJ, 549, 452
Benz, W., Mayor, M., & Mermilliod, J. C. 1984, A&A, 138, 93
Bouvier, J., Forestini, M., & Allain, S. 1997, A&A, 326, 1023
Cudworth, K. M. 1971, AJ, 76, 475
Duvall, T. L., Dziembowski, W. A., Goode, P. R., Gough, D. O., Harvey, J. W., & Leibacher, J. W. 1984, Nature, 310, 22
Edwards, S., et al. 1993, AJ, 106, 372
Eff-Darwich, A., Korzennik, S. G., & Jiménez-Reyes, S. J. 2002, ApJ, 573, 857
Endal, A. S., & Sofia, S. 1981, ApJ, 243, 625
Geller, A., Mathieu, R. D., Harris, H. C., & McClure, R. 2008, AJ, 135, 2264
Goode, P. R., Dziembowski, W. A., Korzennik, S. G., & Rhodes, E. J. 1991, ApJ, 367, 649
Gough, D. O. 1982, Nature, 298, 334
Herbst, W., Eislöffel, J., Mundt, R., & Scholz, A. 2007, in Protostars and Planets V, ed. B. Reipurth, D. Jewitt, & K. Keil (Tucson, AZ: Univ. Arizona Press), 297
Herbst, W., & Wittenmyer, R. 1996, BAAS, 28, 1338
Honeycutt, R. K. 1992, PASP, 104, 435
Horne, J. H., & Baliunas, S. L. 1986, ApJ, 302, 757
Jianke, L., & Collier Cameron, A. 1993, MNRAS, 261, 766
Kalirai, J. S., Fahlman, G. G., Richer, H. B., & Ventura, P. 2003, AJ, 126, 1402
Kawaler, S. D. 1988, ApJ, 333, 236
Kawaler, S. D. 1989, ApJ, 343, L65
Koenigl, A. 1991, ApJ, 370, L39
Kraft, R. P. 1967, ApJ, 150, 551
Krishnamurthi, A., Pinsonneault, M. H., Barnes, S., & Sofia, S. 1997, ApJ, 480, 303
Lockwood, G. W., Thompson, D. T., Radick, R. R., Osborn, W. H., Baggett, W. E., Duncan, D. K., & Hartmann, L. W. 1984, PASP, 96, 714
MacGregor, K. B., & Brenner, M. 1991, ApJ, 376, 204
Mathieu, R. D. 2000, in ASP Conf. Ser. 198, Stellar Clusters and Associations: Convection, Rotation, and Dynamos, ed. R. Pallavicini, G. Micela, & S. Sciortino (San Francisco, CA: ASP), 517
McNamara, B., & Sekiguchi, K. 1986, AJ, 91, 557
Meibom, S., Barnes, S. A., Dolan, C., & Mathieu, R. D. 2001, in ASP Conf. Ser. 243, From Darkness to Light: Origin and Evolution of Young Stellar Clusters (San Francisco, CA: ASP), 711
Meibom, S., & Mathieu, R. D. 2005, ApJ, 620, 970
Meibom, S., Mathieu, R. D., & Stassun, K. G. 2006, ApJ, 653, 621
Meys, J. J. M., Alphenaar, P., & van Leeuwen, F. 1982, Inf. Bull. Var. Stars, 2115, 1
Najita, J. 1995, in RevMexAA Conf. Ser., 1, 293
Nordhagen, S., Herbst, W., Rhode, K. L., & Williams, E. C. 2006, AJ, 132, 1555
Perryman, M. A. C., et al. 1998, A&A, 331, 81
Pinsonneault, M. H., Kawaler, S. D., & Demarque, P. 1990, ApJS, 74, 501
Pinsonneault, M. H., Kawaler, S. D., Sofia, S., & Demarque, P. 1989, ApJ, 338, 424
Prosser, C. F., et al. 1995, PASP, 107, 211
Radick, R. R., Thompson, D. T., Lockwood, G. W., Duncan, D. K., & Baggett, W. E. 1987, ApJ, 321, 459
Rucinski, S. M. 1997, AJ, 113, 1112
Scargle, J. D. 1982, ApJ, 263, 835
Schatzman, E. 1962, Ann. Astrophys., 25, 18
Shu, F., Najita, J., Ostriker, E., Wilkin, F., Ruden, S., & Lizano, S. 1994, ApJ, 429, 781
Sills, A., Pinsonneault, M. H., & Terndrup, D. M. 2000, ApJ, 534, 335
Skumanich, A. 1972, ApJ, 171, 565
Soderblom, D. R. 1982, ApJ, 263, 239
Soderblom, D. R., Jones, B. F., & Walker, M. F. 1983, ApJ, 274, L37
Soderblom, D. R., Stauffer, J. R., Hudon, J. D., & Jones, B. F. 1993a, ApJS, 85, 315
Soderblom, D. R., Stauffer, J. R., MacGregor, K. B., & Jones, B. F. 1993b, ApJ, 409, 624
Stassun, K. G., Ardila, D. R., Barsony, M., Basri, G., & Mathieu, R. D. 2004, AJ, 127, 3537
Stassun, K. G., Mathieu, R. D., Mazeh, T., & Vrba, F. J. 1999, AJ, 117, 2941
Stauffer, J. R., Hartmann, L., Soderblom, D. R., & Burnham, N. 1984, ApJ, 280, 202
Stauffer, J. R., & Hartmann, L. W. 1987, ApJ, 318, 337
Stauffer, J. R., Hartmann, L. W., Burnham, J. N., & Jones, B. F. 1985, ApJ, 289, 247
Stauffer, J. R., Hartmann, L. W., & Jones, B. F. 1989, ApJ, 346, 160
Stelzer, B., et al. 2003, A&A, 411, 517
Terndrup, D. M., Stauffer, J. R., Pinsonneault, M. H., Sills, A., Yuan, Y., Jones, B. F., Fischer, D., & Krishnamurthi, A. 2000, AJ, 119, 1303
van Leeuwen, F., & Alphenaar, P. 1982, Messenger, 28, 15
Vasilevskis, S., Klemola, A., & Preston, G. 1958, AJ, 63, 387
von Hippel, T., Steinhauer, A., Sarajedini, A., & Deliyannis, C. P. 2002, AJ, 124, 1555
Yi, S. K., Kim, Y., & Demarque, P. 2003, ApJS, 144, 259